


High intensity operation using proton stacking in the Fermilab Recycler to deliver 700 kW of 120 GeV proton beam

Robert Ainsworth¹,* Philip Adamson, Bruce C. Brown¹, David Capista, Kyle Hazelwood, Ioanis Kourbanis, Denton K Morris, Meiqin Xiao, and Ming-Jen Yang
Fermi National Accelerator Laboratory, Batavia, Illinois 60510, USA

 (Received 24 October 2019; revised 8 October 2020; accepted 3 November 2020; published 15 December 2020)

As part of the NOvA upgrades in 2012, the Recycler was repurposed as a proton stacker for the Main Injector with the aim to deliver 700 kW. Since January 2017, this design power has been run routinely. The steps taken to commission the Recycler and run at 700 kW operationally will be discussed. Major improvements include a new collimation system to control transverse losses and diode damper system to damp the resistive wall instability during slip-stacking. Plans for future running will also be discussed.

DOI: [10.1103/PhysRevAccelBeams.23.121002](https://doi.org/10.1103/PhysRevAccelBeams.23.121002)

I. INTRODUCTION

During the long shutdown from May 2012 until September 2013, the Recycler [1] was repurposed from an antiproton storage ring to a proton stacker as part of the NOvA [2] project. The design goal for the NOvA project was to deliver a 700 kW proton beam. Before the shutdown, the maximum power sent was 400 kW by slip-stacking in the Main Injector (MI). Converting the Recycler to stack protons meant the beam power at 120 GeV could be increased by reducing the cycle length. This was done by moving the slip-stacking [3,4] process from the Main Injector [5] in to the Recycler such that the Recycler and Main Injector cycles could be overlapped allowing the MI to ramp up and down at its maximum rate.

Figure 1 shows the Fermilab accelerator complex [6]. An ion source [7] produces H^- which are accelerated to 400 MeV in a normal conducting linac. Upon injection into the Booster, charge stripping is used to convert the H^- to protons. The Booster operates on a 15 Hz sinusoidal ramp accelerating protons to 8 GeV before delivering them to either the Recycler for high energy neutrino experiments and the muon campus or the Booster Neutrino Beam (BNB) experiments.

For the high energy neutrino experiments, the Booster sends twelve batches in to the Recycler. The Recycler performs slip-stacking at 8 GeV which doubles the bunch intensity and then delivers beam to the Main Injector where it is accelerated to 120 GeV and sent to NuMI [8]. The

design goal for the NOvA project is for a 700 kW proton beam (48.6×10^{12} protons per pulse (ppp) every 1.333 s.) Figure 2 shows the relative timing of Booster, Recycler, and Main Injector cycles. The advantage of the new scheme can be seen clearly as the Recycler is already stacking beam ready for the next NuMI pulse before the previous pulse has been extracted from the MI.

The Recycler also stacks lower intensity beam which is sent to the MI for resonant extraction and delivered to experiments via Switchyard. The Recycler also rebunches protons from 53 MHz buckets to 2.5 MHz buckets to be sent to the muon campus [9]. Direct injection from the Booster to the Main Injector is also possible and used when there is an issue with the Recycler. In this case, beam can still be delivered to NuMI but at a lower power.

For this new scheme to be successful, the Recycler needed to be repurposed from an antiproton storage ring to a proton stacker. This paper will detail the upgrades needed

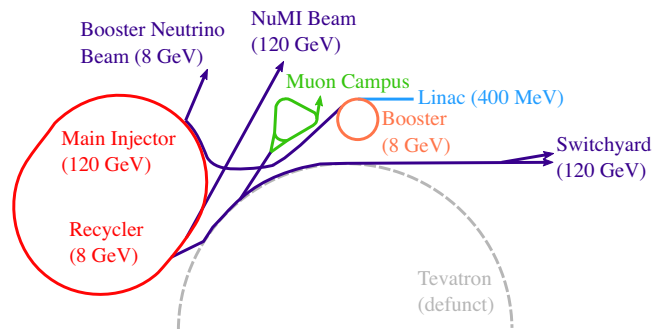


FIG. 1. The Fermilab accelerator complex. H^- are produced at the ion source and accelerated to 400 MeV in a normal conducting linac. These H^- are stripped to protons upon entry into the Booster where they are accelerated to 8 GeV. Twelve Booster batches are then injected into the Recycler where they are slip-stacked to form six double intensity batches. These batches are then accelerated to 120 GeV in the Main Injector.

* rainswor@fnal.gov

Published by the American Physical Society under the terms of the *Creative Commons Attribution 4.0 International license*. Further distribution of this work must maintain attribution to the author(s) and the published article's title, journal citation, and DOI.

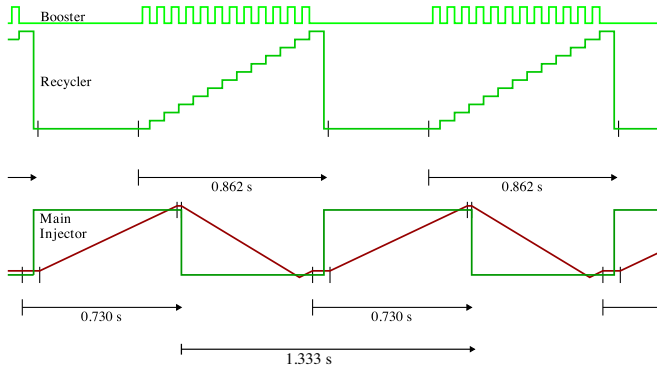


FIG. 2. Relative timing of Booster, Recycler and Main Injector cycles for NOvA-era operations. The beam present in each machine is shown along with the Main Injector momentum ramp in red.

to make this happen and the challenges encountered to realize the 700 kW beam power design goal. The most significant challenge was to increase beam intensity while keeping losses to a minimum. Reusing the Recycler as a proton stacker came with its own set of challenges as it was never designed for this purpose. Examples of these challenges are that the beam pipe is smaller compared Main Injector, there are welds at high beta locations and that the magnets are smaller which means less shielding and thus, more residual activation for the same loss. It is crucial to maintain losses to a minimum such that the tunnel and components remain serviceable. Loss limits are based on typical running which is known to have acceptable levels of residual radiation in the tunnel. Radiation surveys are carried out on a regular basis (typically once a month) to confirm residual radiation levels match expectations.

II. RECYCLER UPGRADES

The Recycler is a permanent magnet ring consisting of strontium ferrite gradient magnets [10] and strontium ferrite quadrupoles [11] in the straight sections. Figure 3 shows a schematic of the Recycler ring. The Recycler shares the same tunnel as the Main Injector and the locations share the same half-cell location names as the Main Injector. The Recycler is split into 6 sections; 100, 200, 300, 400, 500, and 600 where each section contains between 30 and 41 half-cell locations. In order to change the machine tune of the Recycler, a tune trombone [12] is used. The tune trombones are located from 601-609 and 301-309. At each of these half-cell locations, there are four powered quadrupoles which allow a tune variation of up to ± 0.5 . To convert the Recycler from an antiproton storage ring to a proton stacker, a number of upgrades were required [13] which will be described in the following sections.

A. Lattice

Lattice modifications were needed for the Recycler to function as a proton stacker. The removal of the electron

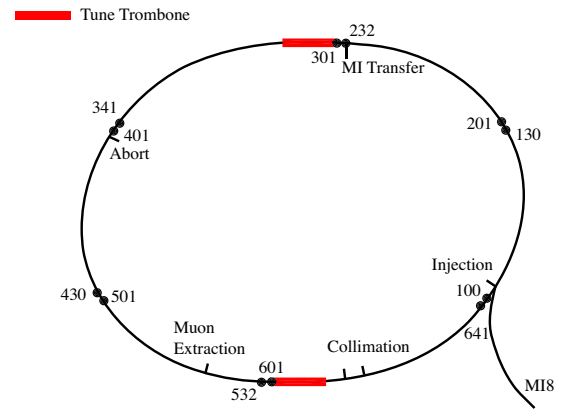


FIG. 3. A schematic of the Recycler with injection and extraction areas labeled. The collimation system was added during the 2016 summer shutdown.

cooling system left space to provide a FODO focusing lattice similar to the rest of the Recycler in place of the electron cooling (ecool) medium beta insert [14]. Eight half cells from 301-309 were rebuilt by removing permanent quadrupoles and installing new permanent quadrupoles which had been fabricated prior to the long shutdown. An additional tune trombone was provided here to permit intensity-dependent tune control. Additional trim sextupoles were installed around the Recycler with the goal of allowing greater control of chromaticity. End shims in the gradient magnets were changed [15,16] in order to provide the desired tune and to meet the goal of allowing chromaticity control between -5 to -20 while keeping the trim sextupoles below a current limit of 5 A. The 301-309 lattice design employed quadrupoles with strength limited by previous successful Recycler magnets. Modifications to the end shims for regular cell gradient magnets provided adequate focusing.

B. Transfer lines

Injection of protons directly from the Booster is accomplished using a new transfer section [17] while maintaining the previous options of beam to the Booster Neutrino Beam and the Main Injector. A pulsed vertical bend directs the protons into a new beamline segment which ends with a Lambertson magnet at 102 and a radial kicker system at 104. A tail bumper magnet is employed to reduce emittance growth for beam in Recycler bunches already in the ring. For transfer from the Recycler to the Main Injector, the new transfer line [18] with improved admittance includes a new full-turn kicker at 230, an MLAW (wide aperture Main Injector Lambertson) Lambertson magnet at 232 followed by mirror magnets at the 301 upstream location as required to permit the circulating and extracted beam aperture needed. In the abort region, the gap clearing kickers [19,20] were repositioned into the Recycler. New full-turn abort kickers and a new MLAW abort Lambertson magnet were installed.

C. rf and instrumentation

A 53 MHz rf system [21] to support bucket-to-bucket transfers from Booster and to Main Injector was needed. A pair of cavities which could be tuned to the injection frequency and 1260 Hz lower were needed for slip-stacking. A spare cavity was also installed. Beam position monitors (BPM's) [22] use the existing detectors but employ new tunnel-to-service building cables and electronics re-purposed from the Tevatron system. Horizontal and vertical ion profile monitors (IPMs) [23] were installed to allow monitoring of beam properties at high intensity. For controlling resistive wall instabilities, bunch-by-bunch dampers similar to the Main Injector system [24] were added so that high chromaticity would be needed only when slipping bunches overlapped. A dc current transformer (DCCT) and several toroids were added to monitor beam intensities.

D. Vacuum

When the Recycler was used as an antiproton storage ring, ultrahigh vacuum of 1×10^{-10} torr (1.3×10^{-8} Pa) or better was required. This was provided using titanium sublimation pumps (TSPs). Ultrahigh vacuum levels are no longer needed now that the beam is in the machine for less than a second so it was decided to replace the TSPs with ion pumps to match the vacuum design of the Main Injector. One of the major disadvantages of TSPs is that they are consumable and were nearing their end of life. Another disadvantage is that the beam pipe had to be baked after breaking vacuum to remove any absorbed water. Higher intensity running would also lead to more desorption and further decrease the TSPs lifetime.

A total of 600 pumps were installed during 3 summer shutdowns in which the vacuum ports were welded onto the existing TSP cans. The vacuum is now maintained around the 1×10^{-8} torr (1.3×10^{-6} Pa) level. The vacuum system also allowed the ability to perform fast scrubbing.

E. Upgrades to other machines

Upgrades to other machines were also required to achieve the goal of 700 kW. By using the Recycler for stacking, the Main Injector cycle time is reduced to 1.5 sec increasing the beam power from 392 kW to 628 kW (a factor of 1.47 because of the cycle reduction and a factor of 1.09 because of the intensity increase). To further decrease the Main Injector cycle time to 1.333 sec and thus increasing the power to 705 kW, the maximum acceleration rate was increased from 204 GeV/sec to 240 GeV/sec. In order to accommodate the faster ramp, one of the quad power supplies was upgraded and two extra rf stations were added.

III. PERFORMANCE

Since January 2017, the Fermilab accelerator complex (Fig. 4) has been run at the design goal of 700 kW consistently. Some typical Recycler properties for beam sent to NuMI in 2018 are shown in Table I.

Figure 4 shows the evolution of the NuMI beam power since end of the long shutdown in 2013 until July 10th 2019. The power is initially limited to 240 kW in which only the Main Injector is used. Slip-stacking in the Recycler was commissioned in multiple phases as “2 + 6,” “4 + 6,” and “6 + 6” in which the first number represents the number of batches that are slipped. “6 + 6” slip-stacking

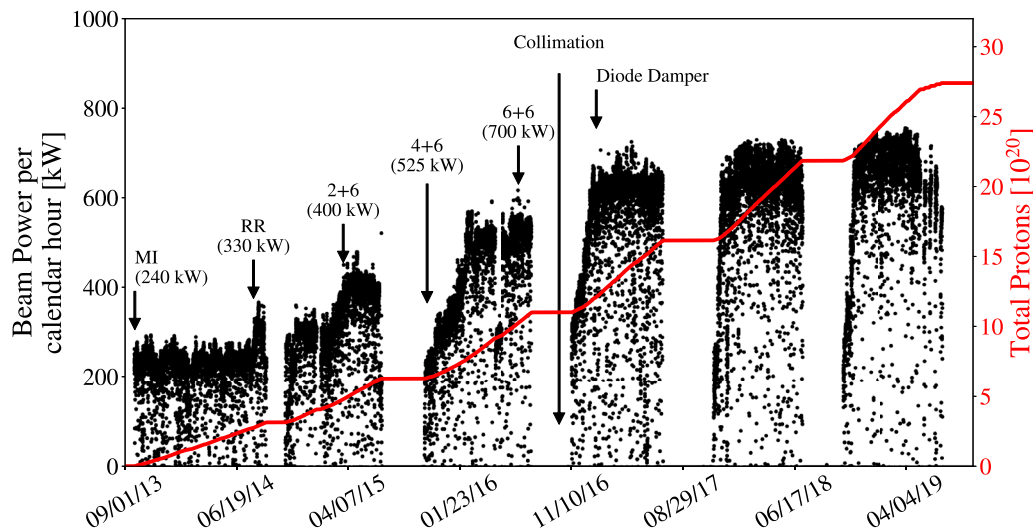


FIG. 4. The hourly beam power to NuMI and the total protons delivered since the end of the long shutdown in 2013. The beam power is initially limited to 240 kW when only the Main Injector is used. As slip-stacking in the Recycler is commissioned, the beam power is steadily increased until January 2017 when the beam power meets the design goal. If beam is also being delivered to Switchyard via resonant extraction in the Main Injector, NuMI will see a 10% decrease in beam power (630 kW).

TABLE I. Typical Recycler properties for beam sent to NuMI with an average power of 700 kW.

Parameter	RR	unit
Q_h	25.42	
Q_v	24.42	
ξ_h	-6	
ξ_v	-7	
$\epsilon_{n,95\%}$	15	π mm mrad
$\epsilon_{L,95\%}$	0.08	eV s
Intensity	5×10^{10}	ppb
V_{RF}	80	kV

was established just prior to the 2016 summer shutdown in which twelve batches from the Booster are injected into the Recycler which are slip-stacked to make six double intensity batches.

The Recycler ring can accommodate seven Booster batches, being 7 times the circumference of the Booster. However, for slip stacking, a gap equal to the Booster batch length is needed for injection. Slip-stacking works by injecting 6 batches, known as group A, at the design momentum of the Recycler ring. These 6 batches are then decelerated by $\Delta f = 1260$ Hz which is given by the product of the Booster harmonic number (84) with the Booster cycle rate (15 Hz). This frequency is chosen such that group A slips by one batch length in one 15 Hz cycle. Six more batches, known as group B, are then injected on-momentum. The decelerated batches will then slip with respect to these on-momentum batches. Near the end of the cycle, both groups are accelerated by 630 Hz in order to optimize the aperture. When the two sets of six batches are overlapped, they are extracted to the Main Injector which recaptures the bunches in its 53 MHz rf system with a capture voltage of 1 MV. The slip-stacking procedure results in beam lost from the bucket due to deceleration and the beating of the two RF systems running at different frequencies. Gap clearing kickers are fired just before each injection and once after extraction in order to abort any out-of-bucket beam in the gap. Any out-of-bucket beam that makes it into the Main Injector is controlled with the existing Main Injector collimation system [25]. In order to damp the resistive wall instability, a bunch-by-bunch damper system is used which damps the two sets of six batches individually. However, when the batches begin to overlap, this system no longer works as it is unable to resolve the individual bunches positions. Therefore with no damper during this time (around the seventh injection), the chromaticity is increased to stabilize the beam against the instability. At high intensities, a large chromaticity of -20 is required at the end of the cycle which results in a new set of issues.

Running with high chromaticity resulted in uncontrolled losses around the ring due to emittance growth, especially at the tight aperture Lambertson magnet locations.

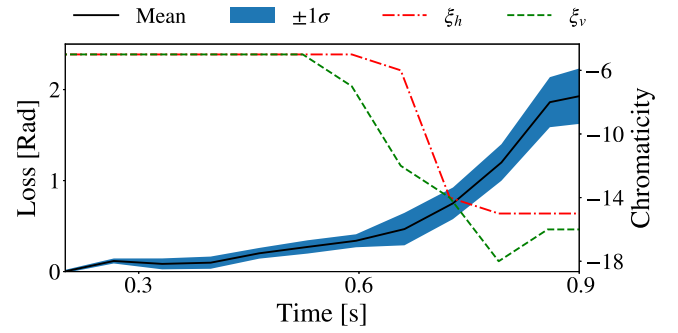


FIG. 5. An example of how the total loss sum increase with chromaticity before the installation of the diode damper. The black line shows the average of 100 pulses along a blue band showing one standard deviation from this mean.

A second issue is a much more constrained tune space. The decelerated bunches during slip-stacking have a tune offset compared to the set machine tune caused by chromaticity which to first order is $\sim \frac{\partial Q}{\partial p} \xi$. The larger the chromaticity, the larger the tune offset. At -7 chromaticity, this offset is $dQ = 0.018$ compared to $dQ = 0.054$ for -20 chromaticity. This meant that as the chromaticity was increased, the set tune of the machine was lowered to prevent the off-momentum beam being pushed toward the half-integer resonance [26]. Figure 5 shows how the losses increased exponentially as the chromaticity was increased during a “4 + 6” cycle. The black line shows the average of 100 pulses along with a one standard deviation band (blue shading). In order to reduce this problem, the tune was lowered as the chromaticity was increased.

It was found that by introducing an rf injection phase offset on the first six injected batches in order to reduce the peak current of these bunches, the final chromaticity could be reduced by 2 or 3 units. The injection offset resulted in more beam in the gap however this could be controlled cleanly with the gap clearing kickers rather than losing beam around the ring. Figure 6 shows the beam injected into the Recycler and how much survives. Around

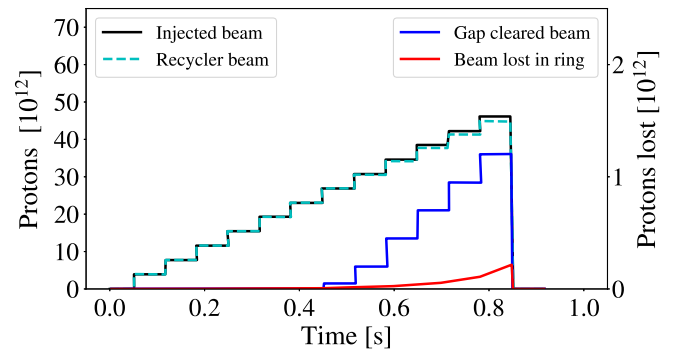


FIG. 6. The beam injected (left scale) into the Recycler during a “6 + 6” cycle along with the gap cleared beam and beam lost (right scale) in the ring in 2016.

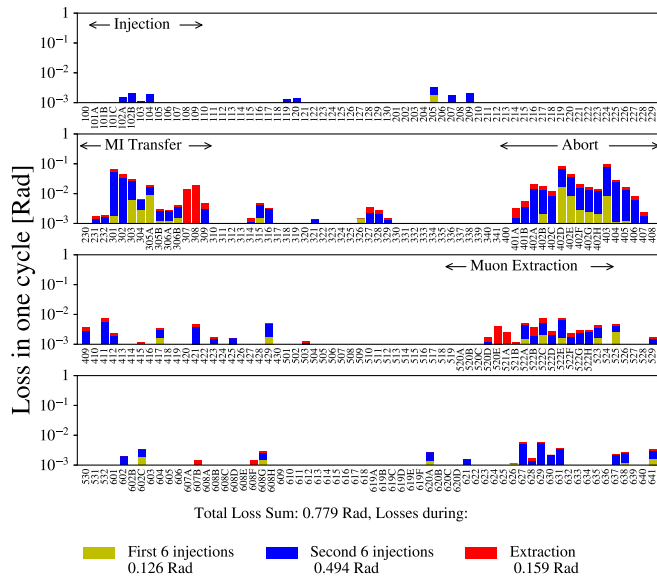


FIG. 7. Typical loss pattern around the Recycler before the 2016 summer shutdown. Intensity is 42×10^{12} ppp.

1.2×10^{12} is sent to the abort using the gap clearing kickers and $\sim 2 \times 10^{11}$ is lost around the ring. The beam lost to the ring shows a nonlinear increase toward the end of cycle caused by the high chromaticity running.

The Recycler shares the same beam loss monitoring system as the Main Injector. A ionization chamber beam loss monitor (BLM) is located at each half-cell location. Extra BLMs are added at locations of interest such as Lambertson magnet locations or at collimators. Figure 7 shows a typical loss pattern in Rad during one machine cycle around the Recycler before the 2016 summer shutdown. Each subplot represents a different section of the Recycler ring and each bar corresponds to a different loss monitor. The different colour of the losses determine when the loss happened during the cycle. Yellow is during the first 6 injections, blue is the second six and red is during extraction. The worst losses occur at the Lambertson magnet locations used to extract beam to the Main Injector located at 232 and the abort Lambertson magnet located at 402. The majority of the loss at 402 is caused by the tails of the gap clearing kickers which are fired 13 times a cycle. In order to run 700 kW consistently, the transverse losses needed to be controlled better.

IV. COLLIMATION

The Recycler was originally purposed to store antiprotons. As such, its aperture is smaller than that of the Main Injector. Since the Recycler began stacking protons, aperture restrictions were a big concern. In addition, the design of the machine meant that the maximum beta was placed between magnets which meant residual radiation in those

areas would be more problematic. Several areas were addressed trying to fix problems related to faulty welds or poor alignment. However, this was not sufficient and so a collimation system was needed to control losses.

Longitudinal losses from slip-stacking are already controlled using gap clearing kickers and collimation in the Main Injector. During the 2016 summer shutdown, a two-stage collimation system [27] was installed in the Recycler to take care of uncontrolled transverse losses. The system consists of a primary scraping foil edge, and two large, 20 ton secondary collimators made from steel and marble. Each secondary collimator is followed by a downstream mask to absorb forward scatter. After each injection, a closed vertical bump is used to move the beam edge toward the collimators in order to let the damper system remove any injection errors before the bump.

Figure 8 shows a typical loss pattern around the Recycler after the collimators were installed. It can be seen that the large losses at the MI transfer Lambertson magnet were reduced as well as many small losses around the ring caused by limited aperture.

It can also be seen that the loss sum has increased compared to Figure 7. There is an increase in losses at the collimation system however, beam is lost here in a controlled way. More losses are accepted at the collimator with the benefit of reducing losses around the rest of the machine. Due to the increased shielding around the collimators, although losses have increased, the residual radiation in the tunnel is smaller compared to comparable losses at non collimation areas. If the losses from collimation are removed, the loss sum for the rest of the ring is 0.5 Rad. This loss sum, which includes a 7% intensity increase, is lower than before collimation (0.779 Rad).

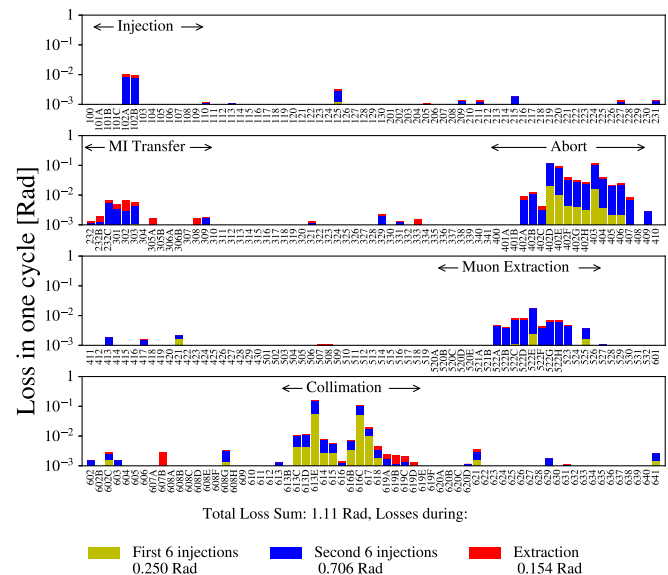


FIG. 8. Typical loss pattern after installing the two stage collimation system. Intensity is around 45×10^{12} ppp.

It should also be noted that extra loss monitors were added at the collimators which are both denser packed than those in the normal locations, and also closer to the Recycler; both these factors increase the scaling of loss to loss monitor counts.

While commissioning the collimators, tests were performed with just the secondary collimators and increased losses were observed at Lambertson magnet locations confirming that a 2 stage system was the most efficient way to operate the collimators.

V. DIODE DAMPER

While the collimators were able to control a large amount of the transverse losses, there was still a loss associated with running very high chromaticity (-20) at the end of the cycle. During the slipping process the bunch-by-bunch damper system is turned off as it is unable to resolve the bunches position while they are overlapping. High chromaticity is therefore needed to suppress the resistive wall instability.

It was proposed by [28] that the slipping motion can be ignored, i.e., bunches in both beams are executing the same motion. Thus a damper system with a 5 MHz bandwidth looking at the envelope of all bunches motion rather than a bunch-by-bunch damper would be sufficient.

The damper system follows a similar idea to that of direct diode detection [29]. The output of pickups are sent through a diode followed by a resistor and capacitor in parallel to form peak detectors which provide an envelope of the bunches motion. The envelope signal is passed through a 3 turn filter with correct coefficients to calculate a kick to damp the beam.

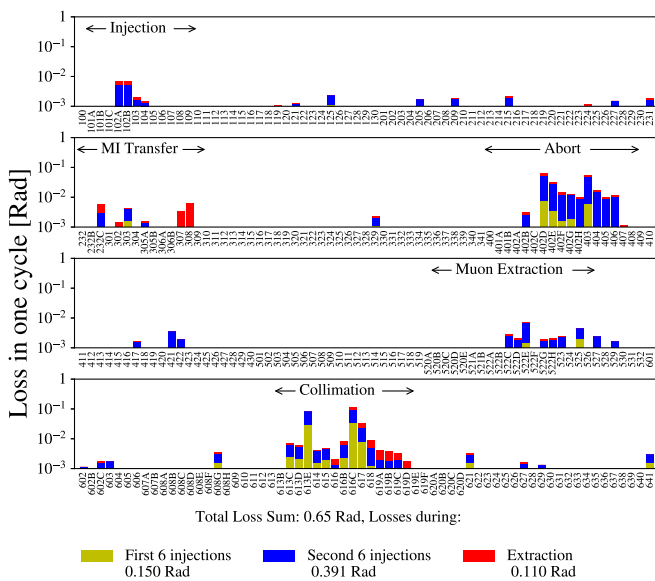


FIG. 9. Typical loss pattern after the implementation of the diode damper which allowed chromaticity to be dropped at the end of the cycle. Intensity is around 45×10^{12} ppp.

The system [30] was successfully implemented in January 2017 and allowed the chromaticity during slipping to be reduced from -20 down to -7. Figure 9 shows the effect of the damper on the loss pattern for the same intensity as in Fig. 8. The total loss sum has reduced by almost a factor of two with losses at the abort and muon extraction Lambertson magnets reduced significantly. The ability to run with much lower chromaticity also provided much more freedom in choosing the working point and to remove the injection phase offsets.

VI. FURTHER APERTURE IMPROVEMENTS

Following these improvements, it can be seen from Fig. 9, the next limiting loss location were at the abort and muon extraction Lambertson magnets. In the 2017 summer shutdown, the permanent magnet Lambertson magnet in the abort region was replaced with a powered Main Injector style Lambertson magnet with improved aperture (MLAW) to help reduce losses in this area. Figure 10 shows aperture for the old permanent magnet Lambertson magnet(left) and the new Main Injector style Lambertson magnet(right) along with solid lines for $\pm 3\sigma$ and dashed lines show $\pm 5\sigma$ for 25 π mm mrad beam. The $\pm 5\sigma$ beam fits comfortably within the Lambertson magnet aperture for the new MLAW. The beam pipe leading into the Muon extraction Lambertson magnet was also replaced with the larger style elliptical pipe used in the Main Injector. The lattice optics were slightly modified using the 30 section tune trombone quadrupoles to help reduce the beta function in the region of the Muon extraction Lambertson magnet. Figure 11 shows the loss patterns after these changes for 700 kW operations. The losses seen at the abort Lambertson magnet are much reduced and now, almost no loss is seen at the muon extraction Lambertson magnet.

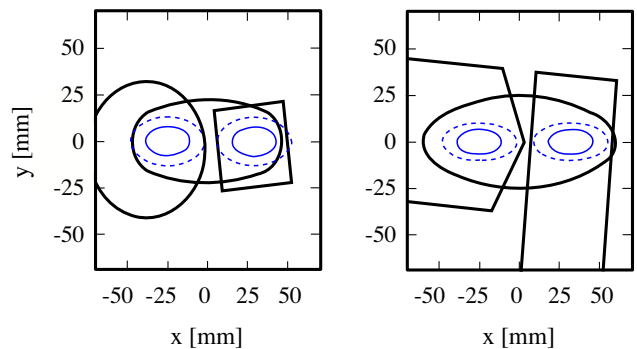


FIG. 10. The aperture sizes for the old Recycler permanent magnet Lambertson magnet (left) and the Main Injector MLAW Lambertson magnet (right). The solid line shows $\pm 3\sigma$ and the dashed line $\pm 5\sigma$ for 25 π mm mrad beam.

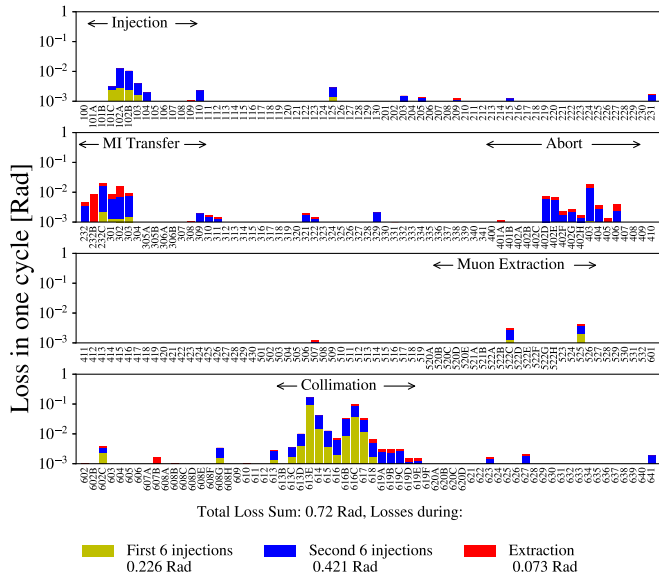


FIG. 11. A typical Recycler loss pattern after the aperture improvements. Intensity is around 50×10^{12} ppp.

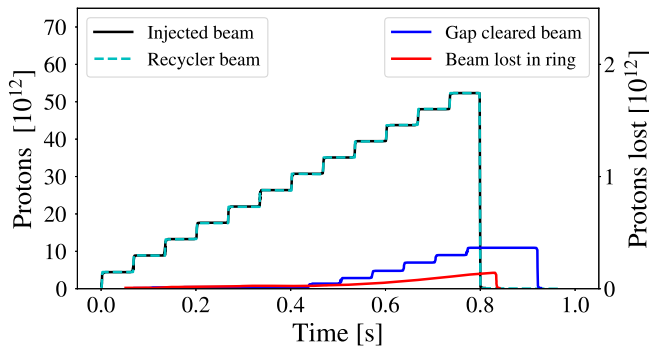


FIG. 12. The beam injected (left scale) into the Recycler during a “6 + 6” cycle along with the gap cleared beam and beam lost (right scale) in the ring in 2018.

VII. CURRENT RUNNING

In 2018-2019, both the Recycler and Main Injector each have an efficiency of around 98.5%. Figure 12 shows a similar plot to Fig. 6. It can be seen that the gap cleared beam is now a factor of 3 smaller than what it was in 2016. This is partly due to the removal of the injection phase offsets and beam injected from the Booster with smaller longitudinal emittance. The losses in the ring are a similar size to before except now more than 2/3 of this is going to the collimators. On April 4, 2019, the record one hour average beam power of 757.75 kW was achieved.

VIII. INSTABILITIES

During commissioning of the Recycler, a fast instability [31] was previously observed which was attributed to electron cloud in which a small fraction of electrons were

trapped in the magnetic field lines of the gradient magnets. This instability has not been observed for some time, most likely due to vacuum scrubbing from the high intensity beam or possibly from the change made to the vacuum system. The secondary electron yield (SEY) stand in the Main Injector allows *in situ* measurements of the SEY of different samples. Measurements of stainless steel showed an initial SEY of 2 which conditioned down to 1.25 [32]. Efforts to induce this instability for study purposes were also unsuccessful.

Other instabilities that occur such as the resistive wall instability are controlled with dampers and do not affect operations.

IX. RADIATION SURVEYS

While running 700 kW consistently, it is important to keep losses controlled and avoid irradiating the tunnel unnecessarily. Ring wide radiation surveys are performed whenever there is an opportunity to access the tunnel using DALE (Data Acquisition Logging Engine). DALE consists of a Geiger counter which has its position recorded by a wheel while attached to the back of a cart. The radiation surveys are important to make sure that our beam loss monitor (BLM) system is not missing any locations. An example survey made on February 6, 2018 shows radiation hot spots around the tunnel measured from the aisle center (Fig. 13). The tunnel houses both the Main Injector and the Recycler so the resulting measurement shows the radiation dose in mRem/hr from both machines. DALE surveys underestimate loss locations where the reading is above 150 mRem/hr. Additional surveys are performed at these points with more accurate equipment [33].

The largest spikes are between 301 and 310 which is the location of the Main Injector collimators. The other locations all match with locations shown in the Recycler loss plots with the exception of a large spike seen at 510. This is a Main Injector loss related to transition crossing when the rf voltage is limited due to tripped stations.

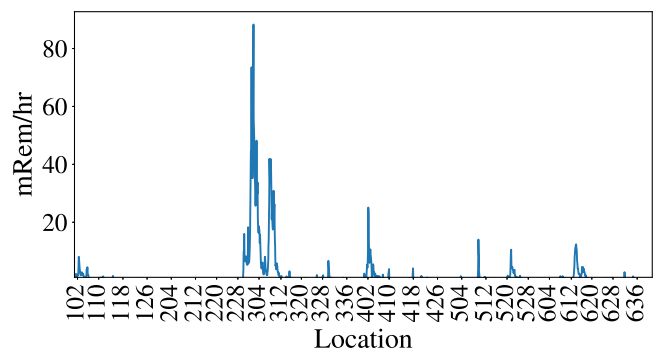


FIG. 13. A DALE survey showing dose rates at locations around the tunnel. Readings are normalized to 1 hour after beam.

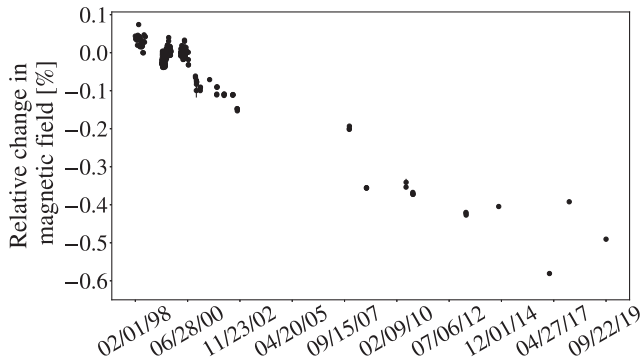


FIG. 14. The relative magnetic field strength of a Recycler style permanent magnet over time.

X. MAGNETIC FIELD DEGRADATION

With the Recycler being a permanent magnet ring, one concern is the magnetic field degradation over time. The original design momentum of the Recycler was 8.889 GeV/C. At the beginning of the NOvA era (January 2014), the momentum on the central orbit was measured to be 8.835 GeV/C, a drop of 0.6%. This agrees well with measurements [34] which are shown in Fig. 14 of a reference magnet which saw a 0.4% drop over a 10 year period which appears to follow the expected logarithmic time dependence [35]. The orbit was remeasured in 2017 and no change of the momentum was required.

XI. SUMMARY AND FUTURE RUNNING

Following a series of improvements, with the most significant being the installation of collimators and a damper system for when beams are slipping, the Fermilab accelerator complex delivers 700 kW consistently to NuMI. In addition to improvements in the Main Injector and Recycler, upgrades to the Booster [36] resulted in better quality beam. We observe that the efficiency in the current configuration is better than 97% compare to < 95% for slip-stacking just in the Main Injector.

The current beam power that can be sent to NuMI is not limited by beam physics but by administrative limits. A new shielding assessment in 2018 meant the Main Injector could deliver more protons per hour however, there was a limit of 54×10^{12} ppp on the NuMI target. During the 2019 summer shutdown, the NuMI target was replaced and the per pulse intensity limit has been increased to 65×10^{12} . However, the beam power is still limited to 777 kW until the horn is replaced, which is scheduled to happen in the 2020 summer shutdown. Studies are already under way looking at potential issues at higher intensity. In-depth simulations are already underway looking a potential problems from space charge. In the 2018 summer shutdown, dedicated sextupoles were installed to allow compensation of the $3Q_x = 76$ resonance to open up the tune

space. Lattice optimization is underway to move the lattice functions as measured much closer to the design values.

The Main Injector ramp has recently been shortened from 1.33 s to 1.2 s which will result in a 10% power increase if only the Neutrino experiments are receiving beam. However, when beam is being sent to Muon campus via the Recycler, the Main Injector ramp spacing is set to 1.4 s which limits the beam power.

ACKNOWLEDGMENTS

The authors would like to thank O. Kiemschies for providing the magnet data shown in Fig. 14. This manuscript has been authored by Fermi Research Alliance, LLC under Contract No. DE-AC02-07CH11359 with the U.S. Department of Energy, Office of Science, Office of High Energy Physics.

-
- [1] G. Jackson, The Fermilab recycler ring technical design report: Rev. 1.2, Fermilab Report No. FNAL-TM-1991, 1996.
 - [2] D. S. Ayres *et al.* (NOvA), The NOvA technical design report, Fermilab Report No. FERMILAB-DESIGN-2007-01, 2007.
 - [3] K. Seiya, B. Chase, J. Dey, P. Joireman, I. Kourbanis, and J. Reid, Slip stacking, in *CARE-HHH-APD Workshop on Finalizing the Roadmap for the Upgrade of the CERN & GSI Accelerator Complex (BEAM'07) Geneva, Switzerland, October 1-5, 2007* (2007), pp. 66–70, <https://inspirehep.net/literature/771038>.
 - [4] R. Ainsworth, P. Adamson, J. Amundson, I. Kourbanis, Q. Lu, and E. Stern, High intensity space charge effects on slip stacked beam in the Fermilab recycler, *Phys. Rev. Accel. Beams* **22**, 020404 (2019).
 - [5] B. C. Brown, P. Adamson, D. Capista, W. Chou, I. Kourbanis, D. K. Morris, K. Seiya, G. H. Wu, and M.-J. Yang, Fermilab main injector: High intensity operation and beam loss control, *Phys. Rev. Accel. Beams* **16**, 071001 (2013).
 - [6] M. Convery, M. Lindgren, S. Nagaitsev, and V. Shiltsev, Fermilab accelerator complex: Status and improvement plans, Fermilab Report No. FERMILAB-TM-2693-AD, 2018.
 - [7] P. R. Karns, D. Bollinger, and A. Sosa, Recent operation of the FNAL magnetron H^- ion source, *AIP Conf. Proc.* **1869**, 030055 (2017).
 - [8] P. Adamson *et al.*, The NuMI neutrino beam, *Nucl. Instrum. Methods Phys. Res., Sect. A* **806**, 279 (2016).
 - [9] D. Stratakis, B. Drendel, J. P. Morgan, M. J. Syphers, and N. S. Froemming, Commissioning and first results of the Fermilab Muon Campus, *Phys. Rev. Accel. Beams* **22**, 011001 (2019).
 - [10] B. C. Brown, J. DiMarco, G. W. Foster, H. D. Glass, J. E. Haggard, D. J. Harding, G. P. Jackson, M. P. May, T. H. Nicol, J. F. Ostiguy, P. Schlabach, and J. T. Volk, Hybrid permanent magnet gradient dipoles for the recycler ring at Fermilab, in *Proceedings of 15th International Conference*

- on *Magnet Technology*, edited by S. G. L. Liangzhen and Y. Luguang (Science Press, Beijing, 1998), p. 161, also available as FERMILAB-Conf-97/338.
- [11] B. C. Brown, S. M. Pruss, G. W. Foster, H. D. Glass, D. J. Harding, G. P. Jackson, M. P. May, T. H. Nicol, J. F. Ostiguy, P. Schlabach, and J. T. Volk, Hybrid permanent magnet quadrupoles for the recycler ring at Fermilab, in *Proceedings of 15th International Conference on Magnet Technology*, edited by S. G. L. Liangzhen and Y. Luguang (Science Press, Beijing, 1998) p. 183, also available as FERMILAB-Conf-97/337.
- [12] M. Xiao, Phase trombone program migration for the recycler ring at Fermilab, Conf. Proc. C **0505161**, 3135 (2005), <https://ieeexplore.ieee.org/document/1591389>.
- [13] D. S. Ayres *et al.*, Technical Design Report for CD-2/3a, Fermilab Report No. Nova-doc 2678 v8, 2007.
- [14] W. Wan, C. Gattuso, D. E. Johnson, C. S. Mishra, and J. A. Volk, Design and implementation of the medium-beta insert of the Fermilab Recycler Ring, Conf. Proc. **C0106181**, 3621 (2001), <https://ieeexplore.ieee.org/document/988198>.
- [15] D. E. Johnson, B. C. Brown, G. W. Foster, C. Gattuso, G. P. Jackson, C. S. Mishra, S. M. Pruss, J. T. Volk, and M.-J. Yang, Corrections to the Fermilab recycler focusing with end shim changes, in *Proceedings of the 2001 Particle Accelerator Conference, Chicago*, edited by P. Lucas (IEEE, New York, 2001) also available as FERMILAB-CONF-01-209-E.
- [16] M. Xiao, Recycler chromaticities and end shims for NOvA at Fermilab, Conf. Proc. C **1205201**, 2023 (2012), <https://arxiv.org/abs/1301.6666>.
- [17] D. Johnson and M. Xiao, The conceptual design of a new transfer line from booster to recycler for the fermilab proton plan phase 2 campaign, IEEE Nucl. Sci. Symp. Conf. Rec. 1727 (2007), <https://ieeexplore.ieee.org/abstract/document/4440878>.
- [18] M. Xiao and D. Johnson, The concept design of a transfer line from the recycler to the main injector for the fermilab nova project, *2007 IEEE Particle Accelerator Conference (PAC)* (2007), pp. 1730–1732, <https://ieeexplore.ieee.org/document/4440879>.
- [19] I. Kourbanis, P. Adamson, J. Biggs, B. C. Brown, D. Capista, C. Jensen, G. Krafczyk, D. Morris, D. Scott, K. Seiya, S. Ward, G. Wu, and M.-J. Yang, A gap clearing kicker for main injector, in *Proceedings of the 2011 Particle Accelerator Conference*, edited by T. Satogata and K. Brown (IEEE, New York, 2011), pp. 1870–1872, also available as FERMILAB-CONF-11-185-AD.
- [20] C. Jensen, R. Reilly, and I. Terekhine, Gap clearing kicker magnet for main injector, in *Proceedings of the 23rd Particle Accelerator Conference, Vancouver, Canada, 2009* (IEEE, Piscataway, NJ, 2009), p. TU6RFP077.
- [21] R. Madrak, A new slip stacking RF system for a twofold power upgrade of Fermilab's Accelerator Complex, *Nucl. Instrum. Methods Phys. Res., Sect. A* **758**, 15 (2014).
- [22] R. Webber, J. L. Crisp, P. Prieto, D. Voy, C. Briegel, C. McClure, R. West, S. H. Pordes, and M. Mengel, Fermilab recycler ring BPM upgrade based on digital receiver technology, *AIP Conf. Proc.* **732**, 190 (2004).
- [23] J. Zagel, M. Alvarez, B. Fellenz, C. Jensen, C. Lundberg, E. McCrory, D. Slimmer, R. Thurman-Keup, and D. Tinsley, Third generation residual gas ionization profile monitors at Fermilab, [arXiv:1502.02703](https://arxiv.org/abs/1502.02703).
- [24] P. Adamson, W. Ashmanskas, G. Foster, S. Hansen, A. Marchionni, D. Nicklaus, A. Semenov, D. Wildman, and H. Kang, Operational performance of a bunch by bunch digital damper in the fermilab main injector, Conf. Proc. C **0505161**, 1440 (2005), <https://ieeexplore.ieee.org/document/1590791>.
- [25] B. Brown *et al.*, Fermilab main injector collimation systems: Design, commissioning and operation, in *Proceedings of the 23rd Particle Accelerator Conference, Vancouver, Canada, 2009* (IEEE, Piscataway, NJ, 2009), p. WE6RFP025.
- [26] R. Ainsworth, P. Adamson, K. Hazelwood, I. Kourbanis, and E. Stern, Simulations and measurements of stopbands in the fermilab recycler, in *Proceedings, 7th International Particle Accelerator Conference (IPAC 2016): Busan, Korea, May 8-13, 2016* (JACoW, Geneva, 2016), p. MOPOY010.
- [27] B. C. Brown *et al.*, Fermilab recycler collimation system design, in *Proceedings, 2nd North American Particle Accelerator Conference (NAPAC2016): Chicago, Illinois, USA, October 9-14, 2016* (2017), p. WEPOA16, <https://www.osti.gov/biblio/1329664-fermilab-recycler-collimation-system-design>.
- [28] A. Burov, Coupled-beam and coupled-bunch instabilities, *Phys. Rev. Accel. Beams* **21**, 114401 (2018).
- [29] M. Gasior and R. Jones, High sensitivity tune measurement by direct diode detection, in *7th European Workshop on Beam Diagnostics and Instrumentation for Particle Accelerators (DIPAC 2005) Lyon, France, June 6-8, 2005* (2005), pp. 310–312, <https://inspirehep.net/literature/704279>.
- [30] N. Eddy, B. Fellenz, P. Prieto, and S. Zorzetti, Transverse damper using diodes for slip stacking in the fermilab recycler, in *Proceedings, 6th International Beam Instrumentation Conference, IBIC2017, Grand Rapids, MI, USA* (2018), p. TUPCF21, <https://inspirehep.net/literature/1673508>.
- [31] S. A. Antipov, P. Adamson, A. Burov, S. Nagaitsev, and M.-J. Yang, Fast instability caused by electron cloud in combined function magnets, *Phys. Rev. Accel. Beams* **20**, 044401 (2017).
- [32] Y. Ji, Electron cloud studies at Fermilab, Ph.D. thesis, IIT, Chicago (2019).
- [33] B. C. Brown and G. H. Wu, Measuring correlations between beam loss and residual radiation in the fermilab main injector, in *Proceedings of the 46th ICFA Advanced Beam Dynamics Workshop on High-Intensity and High-Brightness Hadron Beams (HB2010)*, edited by J. Chrin (Morschach, Switzerland, 2010), pp. 391–394, also available as FERMILAB-CONF-10-368-AD, <https://inspirehep.net/literature/873288>.
- [34] O. Kiemschies, Measurements of strontium ferrite hybrid permanent magnet quadrupoles after removal for the fermilab NOvA upgrade in 2012, in *Proceedings, 6th International Particle Accelerator Conference (IPAC*

- 2015): *Richmond, Virginia, USA, May 3-8, 2015* (JACoW, Geneva, 2015), p. WEPTY029.
- [35] J. Volk, B. Brown, G. Foster, W. Fowler, H. D. Glass, and G. Jackson, Time evolution of fields in strontium ferrite permanent magnets, *Conf. Proc. C* **0106181**, 3215 (2001), <https://ieeexplore.ieee.org/abstract/document/988062>.
- [36] F. Garcia, S. Chaurize, C. Drennan, K. Gollwitzer, V. Lebedev, W. Pellico, J. Reid, C.-Y. Tan, and R. Zwaska, Fermilab - The Proton Improvement Plan (PIP), in *Proceedings, 61st ICFA Advanced Beam Dynamics Workshop on High-Intensity and High-Brightness Hadron Beams (HB2018): Daejeon, Korea, June 17-22, 2018* (2018), p. WEP2PO010, <https://inspirehep.net/literature/1689720>.